J Mater Sci (2015) 50:7208–7217
DOI 10.1007/s10853-015-9275-7

Solid heat-expandable polylactide-poly(methyl methacrylate) foam precursors prepared by immersion in liquid carbon dioxide

Yonghoon Yoon[1] · Christopher J. G. Plummer[1] · Jan-Anders E. Månson[1]

Received: 15 April 2015 / Accepted: 18 July 2015 / Published online: 29 July 2015

Abstract Solid heat-expandable foam precursors were prepared by impregnating melt-blended poly(D,L-lactide) (PDLLA)-poly(methyl methacrylate) (PMMA) blends with liquid carbon dioxide (CO_2). The phase behavior of these blends was strongly dependent on the processing steps, but impregnation with liquid CO_2 led to phase separation regardless of the prior thermomechanical history, and crystallization in blends containing a low-D grade of PDLLA suppressed subsequent expansion. On the other hand, blends containing nominally amorphous high-D PDLLA were found to be unstable with respect to expansion under ambient conditions when saturated with CO_2. It was therefore necessary to reduce the overall CO_2 content by allowing it to desorb partially at 10 °C immediately after impregnation. Under these conditions, the amorphous PDLLA-50 wt% PMMA precursors were stable at ambient temperature and pressure, and showed peak expansion ratios at significantly higher temperatures than pure PDLLA, thanks to the increase in effective glass transition temperature with increasing PMMA content. It was hence demonstrated that blending with PMMA may provide a convenient means of tailoring the process window for heat-expandable polylactide foams, as well as improved heat stability.

✉ Christopher J. G. Plummer
christopher.plummer@epfl.ch

Yonghoon Yoon
yonghoon.yoon@epfl.ch

Jan-Anders E. Månson
jan-anders.manson@epfl.ch

[1] Laboratoire de Technologie des Composites et Polymères (LTC), Ecole Polytechnique Fédérale de Lausanne (EPFL), Station 12, 1015 Lausanne, Switzerland

Introduction

Polylactide (PLA) is a generic term for a range of biodegradable amorphous and semicrystalline aliphatic polyester thermoplastics derived from annually renewable sources of biomass, which have attracted widespread attention as a sustainable alternative to petroleum-based polymers [1]. There has consequently been substantial effort to develop PLA foams using environmentally friendly physical blowing agents such as CO_2 as a replacement for expanded polystyrene (EPS) [2]. The range of application of PLA nevertheless remains limited by its relatively poor thermal resistance and long-term durability. Its glass transition temperature, T_g, and heat deflection temperature in the amorphous state of about 60 and 50 °C, respectively, are significantly lower than those of PS, for example. Various means of improving the thermal properties of PLA have been considered, including stereo complexation [3], copolymerization, and blending [4]. Blending with one or more relatively high T_g polymers is potentially a particularly straightforward and effective way to tailor the glass transition, provided that the different blend components show adequate compatibility and physical characteristics [5, 6]. One promising candidate for blending with PLA is atactic poly(methyl methacrylate) (PMMA), which is an inexpensive amorphous thermoplastic with a T_g typically around 110 °C, depending on its comonomer content and tacticity. While the behavior of PLA–PMMA blends may vary significantly with molar mass, degree of crystallinity, and processing conditions, they have been demonstrated from calorimetric data to show at least partial miscibility and a composition dependent T_g [6–15]. Moreover, the solubility of CO_2 in PLA–PMMA blends under both sub-critical and super-critical conditions is known to be sufficient to permit its use as a

physical blowing agent for the preparation of low-density foams [11, 16].

The present work stems from our specific interest in the use of liquid CO_2 to prepare PLA–PMMA foam precursors in the form of pellets or granules that are sufficiently stable to allow straightforward handling under ambient conditions, but expand on heating to an adjustable process temperature of around 100 °C to form low-density foams with a significantly higher T_g than unmodified PLA foams. The ultimate aim is to develop sustainable alternatives to EPS suitable for integration into a batch process for the production of foam-core particleboard sandwich structures, which requires not only a foam core with adequate thermal stability, but also a good match between the expansion temperature and the optimum consolidation temperature of the particleboard facings. In what follows, we describe (i) the preparation of model PLA–PMMA foam precursors by melt blending, followed by impregnation with liquid CO_2 based on the literature procedures developed for PLA [2, 17]; and (ii) preliminary studies of the thermally induced foaming behavior of these precursors and the characteristics of the resulting foams.

Experimental

Two different commercial grades of poly(D,L-lactide) (PDLLA), whose density is about 1.25 g/cm^3 in the amorphous state [1], were obtained in pellet form from NatureWorks LLC and will be referred to in what follows as PLA1 and PLA2. PLA1 (weight average molar mass, $M_w = 158{,}000$ g/mol) contained 1.6 % D-isomer and was nominally semicrystalline, while PLA2 ($M_w = 320{,}000$ g/mol) contained 11.6 % D-isomer and was nominally amorphous, although it is known to show limited crystallinity, e.g., after prolonged annealing at temperatures immediately above T_g. An injection molding grade of atactic PMMA (density 1.19 g/cm^3, $M_w \approx 100{,}000$ g/mol) was provided by Evonik Industries AG in pellet form. T_g was determined by differential scanning calorimetry (DSC, TA Instruments Q100) heating scans at 10 K/min on 5–6 mg specimens to be 61.0, 58.3, and 110.3 °C for PLA1, PLA2, and the PMMA, respectively, and the peak melting temperature (T_m) of the as-received PLA1 was 172.1 °C. 99.5 % pure CO_2 from Carbagas AG was used as the blowing agent, and a general-purpose grade of talc from Fisher Scientific was used as a nucleating agent for the foaming studies.

A twin-screw extruder equipped with a pelletizer (Prism TSE 16, Thermo Electron Corporation, 16 mm barrel diameter, *L/D* ratio of 15:1) was used to prepare PDLLA–PMMA blends with different compositions. The feed, melt, and metering temperatures were set to 190, 220, and 210 °C, respectively, and the screw speed was approximately 30 RPM. Prior to processing, the PDLLA was dried overnight at 40 °C in a vacuum oven, and the PMMA was dried for at least 2 h at 90 °C in a convection oven. After blending and pelletizing, the blends were stored in a freezer at −20 °C.

The as-received and blended pellets were dried and compression molded into 1-mm-thick disks with a diameter of 25 mm using a hot press (Fontijne TP 50 with 255 × 255 mm^2 heating platens). In each case, the pellets were placed between polyimide release films in a stainless steel mold and held at 200 °C for 5 min. A nominal hydraulic force of 6 kN, equivalent to a pressure of 0.25 MPa, was then applied at the same temperature for a further 5 min, after which the platens were cooled under pressure to room temperature over approximately 15 min using the integrated water cooling system. 0.5–0.6-mm-thick films were prepared for dynamic mechanical analysis (DMA, TA instruments Q800) using the same procedure. Strips cut from the films were subjected to heating scans from 25 to 150 °C at 3 K/min with a 0.05 % sinusoidal deformation in tensile mode at a frequency of 1 Hz.

Impregnation of the compression-molded disks with liquid CO_2 was carried out at approximately 5 MPa and 10 °C using a high-pressure chamber from Autoclave France equipped with a cooling system. After the required impregnation time had elapsed, the pressure was released at a rate of 0.01 MPa/s in each case. After depressurization, certain specimens were immediately transferred to a high precision balance, and the mass loss due to desorption of the CO_2 was monitored as a function of time at 21 °C [17].

The impregnated disks were foamed by immersing them in a thermostatically controlled silicone oil bath, where they were allowed to undergo free expansion and equilibrate at the temperature of the bath. The resulting morphologies were investigated by scanning electron microscopy (SEM, Philips XLF30-FEG operated at between 1 and 3 kV), and the corresponding mechanical response was evaluated from DMA heating scans on 4–8-mm-sided cubic blocks cut from the foams (scanning range 25–150 °C at 3 K/min with a 0.05 % sinusoidal deformation in compression mode at a frequency of 1 Hz). The foam density was estimated directly from the mass of these blocks.

Results and discussion

Thermal and mechanical properties of the blends

All the compression-molded, extruded, and injected specimens were suggested by DSC heating scans from 20 to 230 °C at 10 K/min to be substantially amorphous, in so

far as the net enthalpy changes in this temperature range were very much less than the reported heat of fusion of fully crystalline poly-L-lactide of 93 J/g [18]. PLA1 nevertheless showed a pronounced cold crystallization exotherm with a peak at about 113 °C, followed by a melting endotherm with a peak at about 170 °C, and approximately the same area as the crystallization peak. As seen from Fig. 1a, the as-blended PLA1-20 wt% PMMA pellets also underwent cold crystallization during the heating scans, in this case with an exothermic peak at about 146 °C, and a melting peak at close to 169 °C. However, while a slight endotherm persisted in PLA1-40 wt% PMMA, there was no evidence of cold crystallization under these conditions at higher PMMA contents.

The data in Fig. 1 also suggested the presence of two glass transitions during the first DSC heating scan of the as-extruded blends, whose estimated mid-point temperatures are given in Table 1 as T_{g1} and T_{g2}, with the subscript 2 denoting the higher transition temperature. The blends with the lowest PDLLA contents showed an endothermic peak immediately above T_{g1}, which was attributed to physical aging, and may have masked a second glass transition in certain cases. However, a single, albeit relatively broad glass transition was observed in all the blends during subsequent cooling at 10 K/min from 230 to 20 °C, as well as in the following second heating scan. As seen from Fig. 2, where the identifiable T_g have been plotted as a function of the PMMA content, the transition temperatures, T_{g12}, measured from the second heating scan were intermediate between T_{g1} and T_{g2}.

For both PLA1 and PLA2, T_{g1} showed a small but significant increase over the T_g of the pure PDLLA as the PMMA content increased, and T_{g2} increased by around 30 K as the PMMA content was raised from 40 to 100 wt%, indicating partial miscibility in the as-extruded specimens [19]. On the other hand, the observation of a single T_g on cooling from 230 °C and during the second heating scan was suggestive of complete miscibility in each case, the evolution of T_{g12} with PMMA content indicating strong plasticization by the PDLLA over the whole composition range. Following Herrera et al. [20], this plasticizing effect could be accounted for empirically using the Breckner equation for a two-component blend [21]:

$$T_g(\phi) = T_{gA} + \left(T_{gB} - T_{gA}\right)\left[(1+k_1)\phi - (k_1+k_2)\phi^2 + k_2\phi^3\right], \quad (1)$$

where ϕ is the volume fraction of component B (the PDLLA in this case), with $k_1 = -0.9$ and $k_2 = 0.4$, as shown in Fig. 2.

These results are at least qualitatively consistent with literature results for PLA–PMMA with comparable M_w

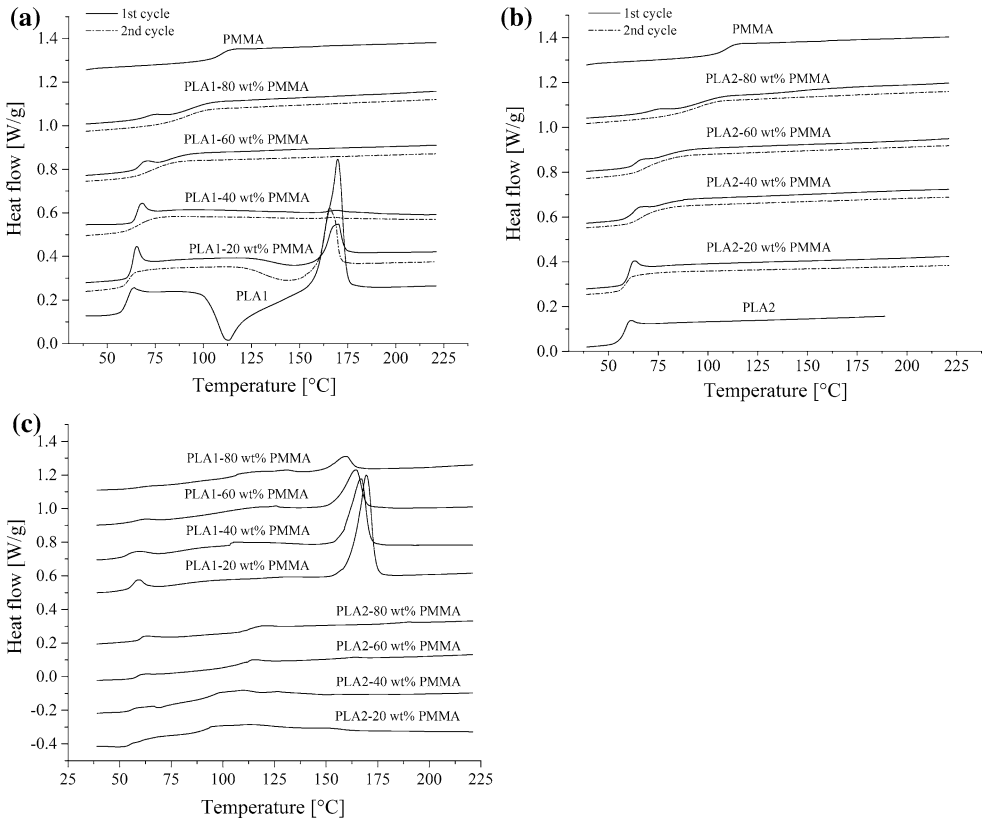

Fig. 1 First and second DSC heating scans of the as-blended **a** PLA1–PMMA blends and **b** PLA2–PMMA blends; **c** DSC heating scans from impregnated compression-molded disks after impregnation for 3 h in liquid CO_2 at 5 MPa and 10 °C, followed by complete desorption of the CO_2

Table 1 Thermal transition temperatures (±0.5 K) and heats of fusion, ΔH, determined by DSC for the different PLA–PMMA blends

wt% PMMA	T_{g1} (°C)	T_{g2} (°C)	T_{g12} (°C)	T_{ma} (°C)	T_{mb} (°C)	ΔH (J/g)
Extruded PLA1–PMMA						
0	60.6			169.9		32.6
20	61.0	–	61.0	170.1	166.2	8.0
40	62.5	77.4	66.1	168.6	168.6	0.5
60	68.0	83.7	73.3	–	–	–
80	71.2	92.4	88.7	–	–	–
100	110.0			–	–	–
Extruded PLA2–PMMA						
0	58.4			–	–	–
20	60.3	–	59.7	–	–	–
40	60.9	78.1	63.3	–	–	–
60	66.5	81.6	72.3	–	–	–
80	71.5	95.7	93.1	–	–	–
100	110.0			–	–	–
Compression-molded PLA1–PMMA						
0	60.6			169.4		29.0
20	58.6	–	617	167.0	165.8	17.0
40	62.8	82.7	65.2	167.2	–	1.7
60	73.4	–	75.5	–	–	–
80	–	95.2	88	–	–	–
100	109.6			–	–	–
Compression-molded PLA2–PMMA						
0	57.5			–	–	–
20	55.3	–	58.3	–	–	–
40	61.0	84.5	63.3	–	–	–
60	68.9	–	72.8	–	–	–
80	–	88.3	92.7	–	–	–
100	109.6			–	–	–
Compression-molded PLA1–PMMA after impregnation						
20	56.3	–	–	169.5		29.5
40	55.6	103.6	–	165.9		20.9
60	58.9	104.7	–	162.8		13.4
80	60.5	105.9	–	159.6		4.9
Compression-molded PLA2–PMMA after impregnation						
20	57.9	89.8	–	–		–
40	56.3	94.1	–	–		–
60	59.2	103.6	–	–		–
80	60.2	109.8	–	–		–

after thermal cycling [12, 14, 15], for which it has been suggested that there exists an upper critical solution temperature (UCST) in excess of 200 °C, depending on the molar mass, composition, and tacticity, such that initially phase-separated blends show a single, broad calorimetric T_g after heating to above the UCST [12, 13]. A broad calorimetric glass transition may nevertheless correspond to distinct effective glass transitions associated with intrinsic variations in the local composition, as has been demonstrated for a range of miscible amorphous polymers by, e.g., thermally stimulated depolarization current experiments [20, 22]. Estimates of the effective local T_g for the PDLLA- and PMMA-rich regions of the specimens showing a single calorimetric T_g are also included in Fig. 2, assuming the same mixing rule as for T_{g12} (Eq. 1) but by replacing the global concentration by the local "self-concentration," following [20] (the characteristic ratios, C_∞, were taken to be 11.7 and about 9 for PDLLA [23] and atactic PMMA [24], respectively). The T_{g1} and T_{g2} of the as-extruded blends were generally well outside this

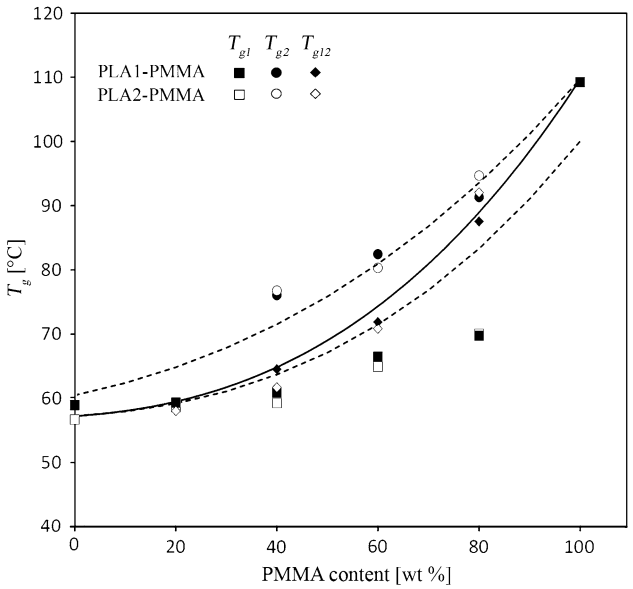

Fig. 2 T_g of the blends estimated from the mid-points of the glass transitions in Fig. 1 as a function of PMMA content. The *solid curve* is a fit to the data from the second DSC heating scans using Eq. (1) and the *hatched curves* are corresponding estimates of the effective local T_g for the PLA- and PMMA-rich regions obtained as described in the main text

envelope at intermediate compositions, confirming macroscopic phase separation to have taken place.

It follows that the present melt blending procedure, for which the extrusion temperatures (maximum 220 °C) and drying conditions were chosen to limit degradation of the PDLLA, was inadequate to give homogeneous blends and, similarly, double glass transitions persisted in the molded specimens (Table 1). For comparison, Samuel et al. [15] have reported melt blending with an extrusion temperature of 210 °C to give homogeneous blends between PLA with $M_w = 218{,}000$ g/mol and PMMA with M_w in the range 92,000–97,000 g/mol. However, they also found phase separation in solvent cast specimens to be irreversible even after heating to 250 °C, implying shear deformation during the extrusion process to be an important factor for the effective miscibility of PLA–PMMA blends. It would therefore be of interest to carry out more systematic studies of the influence of the initial processing conditions on phase separation in the present case. However, in view of the effect of the subsequent CO_2 impregnation step to be discussed below, this was not of immediate practical concern for the preparation of the foam precursors.

DMA results are shown in Fig. 3 for compression-molded films of the pure resins and PDLLA-50 wt% PMMA. The α transition temperatures, T_α, defined as the temperature of the main peak in tan δ were 86.9 and 85.8 °C for PLA1-50 wt% PMMA and PLA2-50 wt% PMMA, whereas the T_α were 69.4, 70.6 ,and 126.2 °C for PLA1, PLA2 ,and PMMA, respectively. PLA1 also showed a marked increase in storage modulus above about 90 °C owing to cold crystallization, but this effect was absent for PLA1-50 wt% PMMA. Consistent with the observation of two glass transitions at 65.5 and 85.1 °C in DSC scans of the films, the DMA transitions for the PLA1-50 wt% PMMA and PLA2-50 wt% PMMA showed relatively small step-like drops in storage modulus at about 67 and 65 °C, respectively, followed by a more substantial decrease as the temperature increased further.

CO_2 impregnation and desorption behavior

Because the CO_2 content stabilized in all the materials for impregnation times in liquid CO_2 at 5 MPa and 10 °C longer than about 3 h, it was assumed to have reached saturation under these conditions, implying equilibrium CO_2 contents of about 0.27, 0.42, and 0.27 g/g for neat PLA1, PLA2, and PMMA, respectively. High CO_2 contents are predicted to reduce T_g of PLA to well below the impregnation temperature of 10 °C [17, 25], facilitating crystallization, and the degree of crystallinity of initially amorphous specimens of PLA1 has been found to be about 34 wt% after impregnation [17, 26]. The difference in the equilibrium CO_2 contents of PLA1 and PLA2 may therefore be accounted for by assuming the CO_2 to be insoluble in the crystalline phase and a simple rule of mixtures. Gas solubility in polymer blends is also expected to follow a simple rule of mixtures [27], as borne out in the present case by the data in Fig. 4. Indeed, the overall equilibrium CO_2 content was roughly independent of composition in the PLA1–PMMA blends, implying phase separation and crystallization of the PLA1 over the whole composition range (and a local CO_2 content in the amorphous regions of the PLA1 that significantly exceeded the global CO_2 content).

As seen from Fig. 1c, DSC heating scans of the blends after impregnation in liquid CO_2 for 3 h, followed by complete CO_2 desorption (which could be achieved e.g., by storage under ambient conditions for a minimum of 1 week [17]), showed two well-separated glass transitions for all the compositions investigated, and T_{g1} and T_{g2} were relatively close to the T_g of the PDLLA and PMMA, respectively (cf. Table 1), indicating significantly greater phase purity than prior to impregnation. Moreover, all the PLA1–PMMA blends showed a clear melting peak, with a single maximum that decreased from 169.5 to about 159.6 °C and a corresponding heat of fusion that decreased from 19.5 to 4.9 J/g as the PMMA content increased from 20 to 80 wt%. Thus, the presence of the CO_2 was confirmed to favor both phase separation and crystallization in the blends at 10 °C, consistent with the observed trends in the overall equilibrium CO_2 content in Fig. 4.

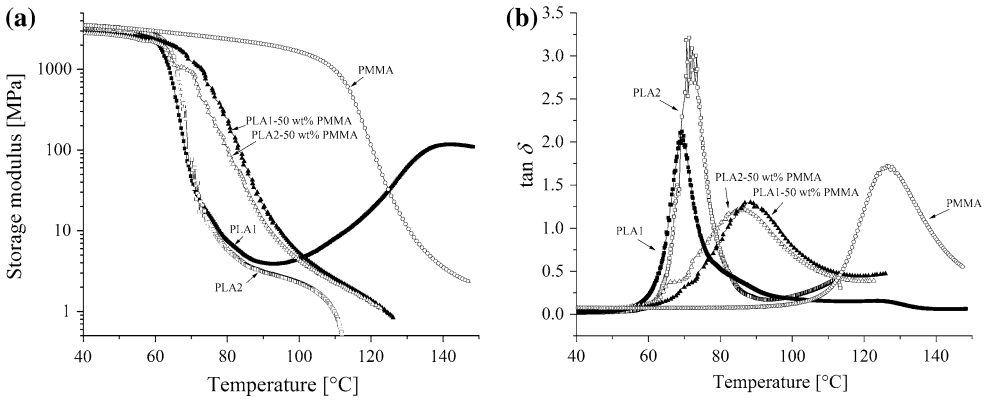

Fig. 3 DMA results from compression-molded films tested in tension: **a** storage moduli and **b** tan δ

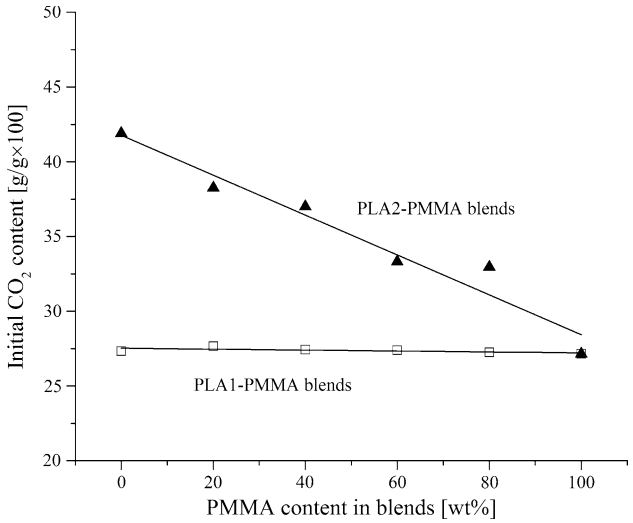

Fig. 4 CO_2 content of compression-molded disks immediately after impregnation for 3 h in liquid CO_2 at 5 MPa and 10 °C as a function of their PMMA content

Figure 5 shows the CO_2 content of the compression-molded disks, expressed as the overall mass of CO_2 per unit mass of the un-impregnated specimens, as a function of time at 21 °C after impregnation for 3 h in liquid CO_2 at 5 MPa and 10 °C. The desorption rates from PLA1, PMMA, and PLA1–PMMA at ambient temperature were comparable, while the PMMA and the PMMA-rich blends showed somewhat greater mass loss after short times; the CO_2 content decreased to about 0.15 g/g in all the specimens after desorption for 1 h and little or no foaming was observed during the measurements. As observed previously [17], crystallization induced by the CO_2 was therefore sufficient to stabilize PLA1 with respect to foaming at temperatures well below its melting point, and estimates of T_g as a function of CO_2 content [25] suggested the glass transition of the PMMA not to decrease to substantially below room temperature, even at saturation. On the other hand, the amorphous PLA2 and its blends with PMMA foamed spontaneously on heating to 21 °C after impregnation, resulting in relatively rapid desorption of the CO_2, particularly at high PLA2 contents, where PLA2-rich regions presumably formed a continuous phase. The blends with intermediate compositions showed the lowest CO_2 contents after desorption for 1 h, owing to both their reduced overall CO_2 contents at saturation and the effect of foaming. Indeed, even PLA2-80 wt% PMMA showed

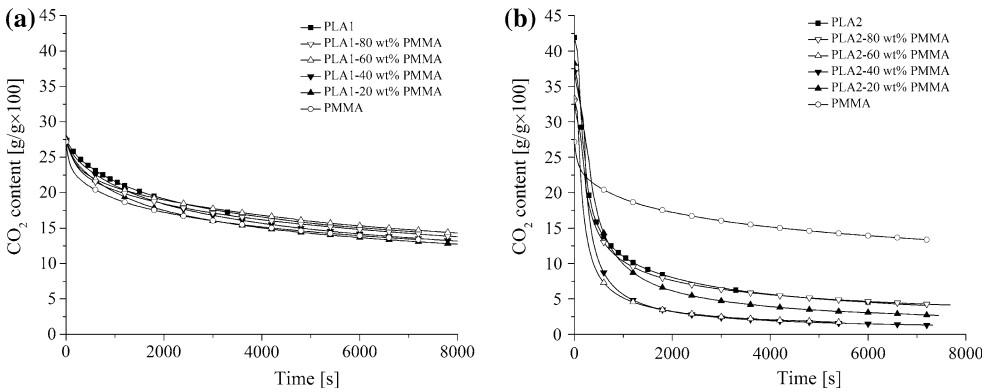

Fig. 5 CO_2 content of compression-molded disks of **a** PLA1–PMMA and **b** PLA2–PMMA and the corresponding homopolymers as a function of time under ambient conditions after impregnation for 3 h in liquid CO_2 at 5 MPa and 10 °C

significantly faster CO_2 desorption than the pure PMMA under these conditions.

Foaming behavior

Only PLA2, PLA2–PMMA, and PMMA were considered for foaming tests, because crystallization of PLA1 and PLA1–PMMA during impregnation tended to suppress foaming not only at ambient temperature, but also in temperature regimes of immediate interest for the direct replacement of EPS. In order to promote relatively homogeneous cellular structures at the scale of the specimen thicknesses, 1 wt% talc was included in the formulations as a nucleation agent. Mineral fillers have been reported to influence the mechanical properties of PLA [28, 29], but this level of loading did not result in significant changes in either mechanical properties or CO_2 transport in the present case. As discussed in the previous section, the amorphous PLA2 and PLA2–PMMA precursors saturated with CO_2 at 5 MPa and 10 °C became unstable with respect to foaming on removal from the autoclave, because of the associated reduction in T_g. It was therefore necessary to modify the impregnation conditions so as to obtain a CO_2 content sufficient to give low-density foams on heating, but low enough to prevent room temperature foaming [17, 30]. Following previous work, the CO_2 content was adjusted by partial impregnation in liquid CO_2 at 10 °C and 5 MPa, followed by conditioning in air at 10 °C and at ambient pressure, which served to homogenize the CO_2 concentration in the specimen interior [17]. Thus, impregnation for 30 min and conditioning for 2 h led to overall CO_2 contents of 0.17 and 0.13 g/g in PLA2 and PLA2-50 wt% PMMA, respectively, whereas impregnation for 2 h and conditioning for 2 h gave an overall CO_2 content of about 0.08 g/g CO_2 in the pure PMMA. For comparison, 0.1 g/g of CO_2 would ideally lead to a minimum bulk foam density close to 20 kg/m^3 assuming expansion of the CO_2 to take place entirely within the foam.

Figure 6 shows the expansion ratio, ρ/ρ^*, where ρ is the matrix density and ρ^* is the foam density, for the above impregnation and conditioning treatments as a function of the foaming temperature, along with SEM micrographs of the resulting cell morphology. Consistent with its relatively high initial CO_2 content, PLA2 generally showed the highest degree of expansion, with ρ/ρ^* reaching a maximum of 56.9 ($\rho^* = 22$ kg/m^3), at 80 °C, falling off as the temperature was increased further. Expansion was reduced for PLA2-50 wt% PMMA owing to its reduced overall CO_2 content, but the maximum in ρ/ρ^* of 18.8 ($\rho^* = 67$ kg/m^3) shifted to 100 °C. Similarly, PMMA showed a maximum in ρ/ρ^* of about 26.1 ($\rho^* = 46$ kg/m^3), at 130 °C.

For PLA2 and PMMA, the maximum in ρ/ρ^* occurred at about $T_g + 20$ °C, where T_g is the glass transition temperature in the absence of CO_2 (Table 1). T_{g1} and T_{g2} were estimated from DSC heating scans (Fig. 7) to be about 64 and 96 °C, respectively, in PLA2-50 wt% PMMA after impregnation and desorption of the CO_2, although the glass transitions were less well defined than for the fully impregnated specimens (cf. Fig. 1c). The weak endotherm visible at 123 °C was also present in DSC heating scans of pure PLA2 after partial impregnation in the presence of talc, and was attributed to residual crystallization (this effect was less evident in the neat PLA2, as seen from Fig. 1). The glass transitions were even less well defined after foaming at 100 °C, as also shown in Fig. 7. In this case, the heat capacity increased gradually over the whole of the temperature range between about 60 and 110 °C, and the endotherm at 123 °C was absent. Finally, a second heating scan of the foams after cooling at 10 °C from 230 °C showed a single broad glass transition centered on about 70 °C. While the relatively complex thermomechanical history and non-uniform exposure to CO_2 of these specimens rendered detailed interpretation of these results difficult, it is speculated that the high strains associated with cell expansion may have promoted homogenization of the matrix microstructures during high temperature foaming, as has been suggested previously for extrusion blending [15]. Certainly, the observation of a maximum in ρ/ρ^* at about 100 °C for the blends implied an effective softening temperature intermediate between those of the pure PLA2 and PMMA.

The SEM micrographs of the various PLA2, PLA2-50 wt% PMMA, and PMMA foams in Fig. 6b were generally suggestive of a mixed open and closed cell morphology; while closed cells appeared to dominate, certain cells were connected via perforations in the cell walls. The apparent maximum cell size increased as the foaming temperature increased in both PLA2 and PLA2-50 wt% PMMA, a trend that was attributed to increasing matrix softening and hence increasing competition between cell growth and/or coalescence, and cell nucleation, there being no simple correlation between the cell sizes and the overall expansion ratio. Moreover, at the highest foaming temperatures, significant shrinkage was observed in the outer regions of the foams subsequent to expansion, presumably because the cell walls were no longer sufficiently rigid to prevent strain recovery associated with the drop in CO_2 pressure towards the end of the expansion process. This led to both an increase in the overall density and inhomogeneous microstructures. The PMMA foams also showed a relatively dense core, implying incomplete penetration of the CO_2 during the impregnation step [17].

The room temperature storage moduli of the foams, E', obtained from compressive DMA tests varied between 0.1 and 50 MPa depending on the foaming temperature and the

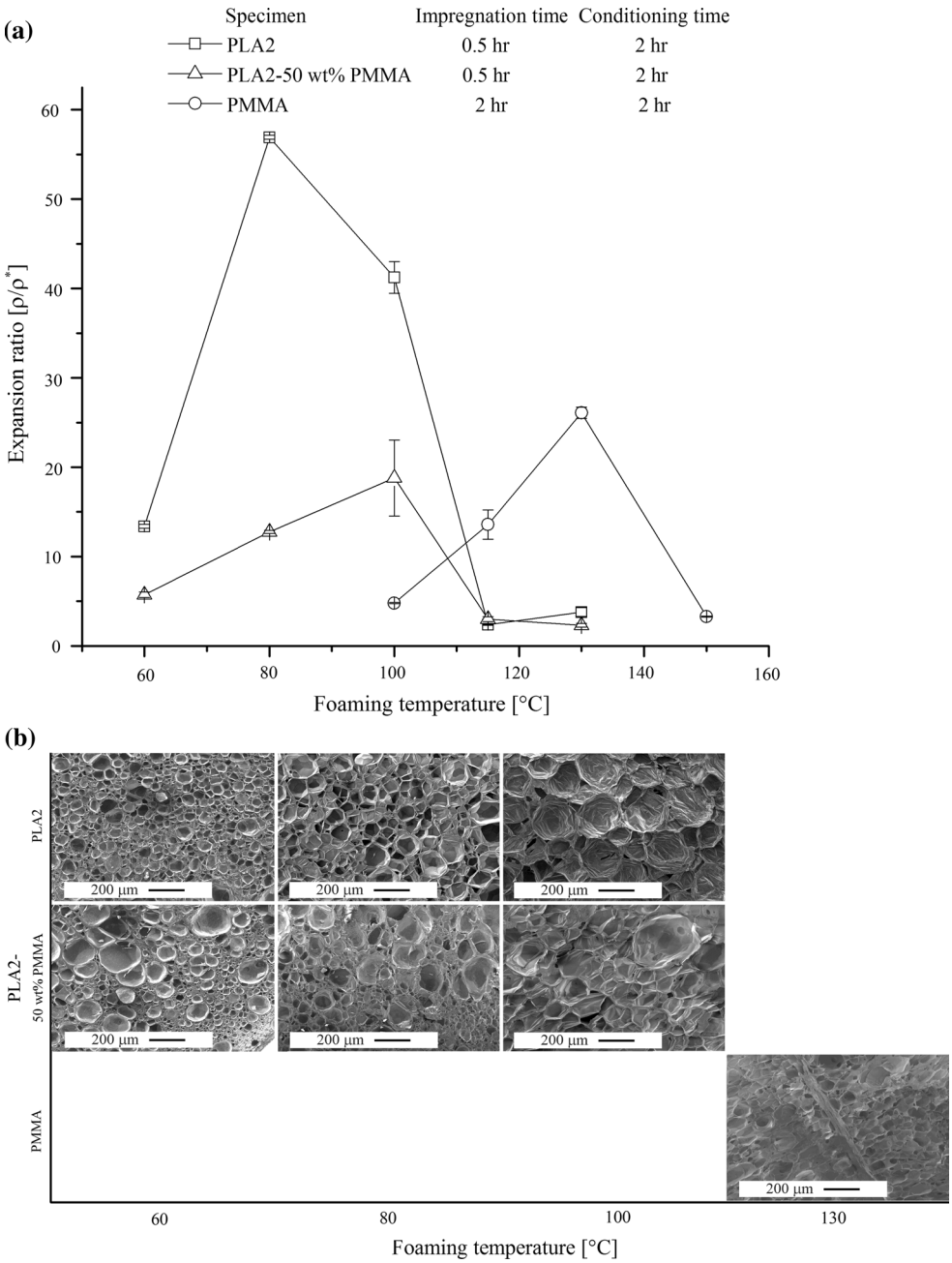

Fig. 6 **a** Expansion ratio, ρ/ρ^* after free expansion of PLA2, PMMA, and PLA2-50 wt% PMMA in a silicone oil bath at various temperatures and for the impregnation/conditioning conditions specified; **b** SEM micrographs of the corresponding foam morphologies

matrix, while the α transition temperatures corresponding to the peak in tan δ (Fig. 8) were broadly consistent with the thermal behavior inferred from the DSC measurements, and the DMA results for the matrices (Fig. 3). Thus, the PLA2-50 wt% PMMA foams showed broad α-transitions with an onset between 60 and 70 °C, but extending to well above 100 °C, such that tan δ reached a maximum at temperatures between 80 and 90 °C, i.e., significantly higher than for the PLA2 foams. Both the PLA2 and PLA2-50 wt% PMMA foams showed significant shrinkage during the measurements, particularly at the lowest foaming temperature, 60 °C, which was reflected by an increase in E' as the temperature approached the onset of the α transition.

Relative moduli, E'/E'_m, where E'_m is the room temperature tensile storage modulus of the corresponding compression-molded specimens (Fig. 3), have been plotted against ρ^*/ρ in Fig. 9. Also shown are simplified Ashby-type scaling laws for a closed-cell foam (linear dependence on ρ^*/ρ) and for an open-cell foam (quadratic dependence on ρ^*/ρ) [31]. The relative moduli were roughly consistent with quadratic scaling, with the exception of the foams produced at 100 °C, for which they were more than an order of magnitude less than would be expected on this

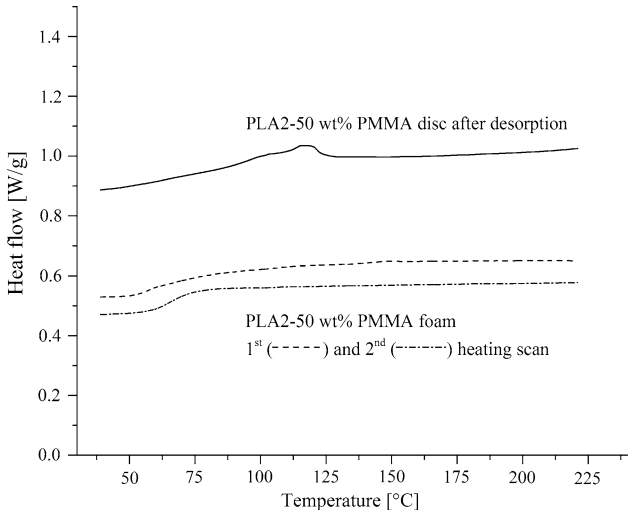

Fig. 7 DSC heating scans from PLA2-50 wt% PMMA after impregnation for 30 min in liquid CO_2 at 5 MPa and 10 °C and conditioning for 2 h at ambient pressure and 10 °C, followed by complete desorption of the CO_2 at room temperature (solid curve); impregnation and conditioning under the same conditions followed by free expansion at 100 °C (hatched curves)

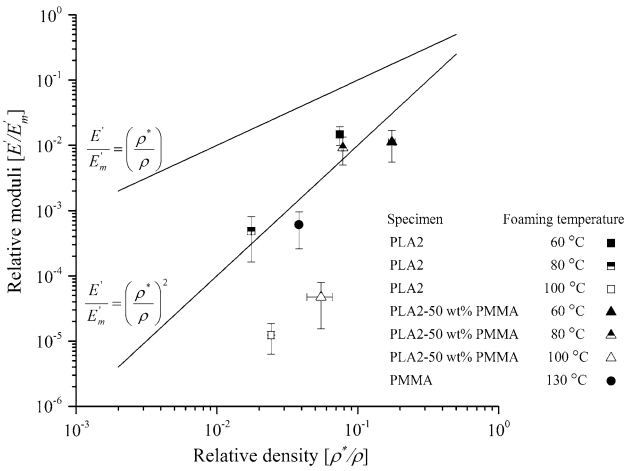

Fig. 9 Relative storage moduli for PLA2, PMMA and PLA2-50 wt% PMMA foams prepared at different foaming temperatures as a function of their relative density

basis. However, as described above, relatively high foaming temperatures resulted in inhomogeneous internal morphologies, so that the overall foam densities were no longer necessarily determinant for the observed compression moduli.

Conclusion

It has been demonstrated that is possible to produce solid-state foam precursors by melt blending of a commercial amorphous high-D PDLLA and PMMA, followed by impregnation with liquid CO_2 and conditioning at ambient pressure in order to adjust the overall CO_2 content. These precursors were shown to be stable with respect to both foaming and short-term CO_2 desorption at room temperature, but could be expanded to form foams with relative densities down to about 0.05 by immersion in a silicon oil bath at temperatures in the neighborhood of 100 °C. The maximum extrusion temperatures for the blends were limited to 220 °C in order to limit degradation of the PDLLA, under which conditions they tended to show two distinct T_g's. Moreover, both DSC and DMA indicated impregnation with liquid CO_2 to result in marked phase separation, obviating efforts to obtain homogeneous blends by prior heat treatment. Even so, the present results indicated that blending PDLLA with PMMA may provide a relatively straightforward means of not only tailoring the process window corresponding to foam expansion, but also increasing the effective softening temperature of the resulting foams. The use of a thermostatically controlled silicon oil bath to initiate expansion in the present case was chosen for convenience rather than to represent a practical processing route, and therefore, no attempt was made to optimize the foam microstructures with respect to blend composition, molar mass, impregnation conditions, precursor geometry, additives, and foaming temperature, for example. However, in ongoing work, we have been able to demonstrate the suitability of granular amorphous PDLLA-50 wt% PMMA precursors impregnated with liquid CO_2

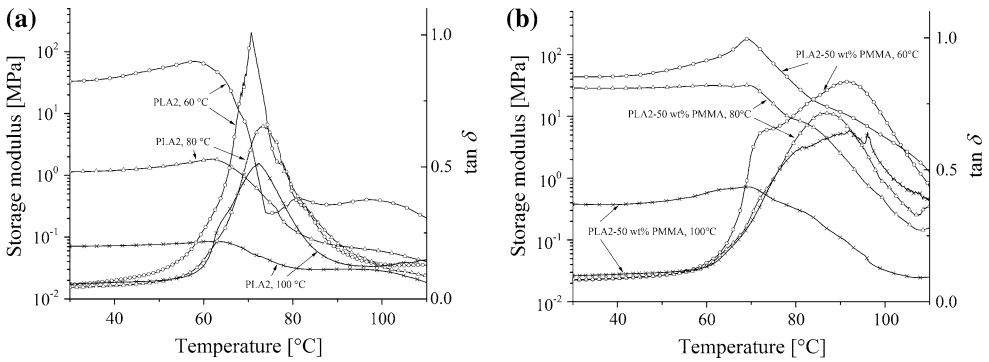

Fig. 8 DMA results from **a** PLA2 and **b** PLA2-50 wt% PMMA foams prepared at different foaming temperatures

for the production of low-density foams using an open hydraulic press in which the foaming temperature is constrained to be close to 100 °C. This will provide the focus for our future efforts towards process optimization.

Acknowledgements We are grateful to the Swiss National Science Foundation for financial support through the program NRP 66 "Resource Wood" and the Interdisciplinary Centre for Electron Microscopy (CIME) of the EPFL for their technical support.

References

1. Garlotta D (2002) A literature review of poly(lactic acid). J Polym Environ 9:63–84
2. Parker K, Garancher JP, Shah S, Fernyhough A (2011) Expanded polylactic acid—an eco-friendly alternative to polystyrene foam. J Cell Plast 47:233–243
3. Ikada Y, Jamshidi K, Tsuji H, Hyon SH (1987) Stereocomplex formation between enantiomeric poly(lactides). Macromolecules 20:904–906
4. Rasal RM, Janorkar AV, Hirt DE (2010) Poly(lactic acid) modifications. Prog Polym Sci 35:338–356
5. Imre B, Pukánszky B (2013) Compatibilization in bio-based and biodegradable polymer blends. Eur Polym J 49:1215–1233
6. Imre B, Renner K, Pukánszky B (2014) Interactions, structure and properties in poly (lactic acid)/thermoplastic polymer blends. Express Polym Lett 8:2–14
7. Samuel C, Cayuela J, Barakat I, Müller AJ, Raquez J-M, Dubois P (2013) Stereocomplexation of polylactide enhanced by poly(-methyl methacrylate): improved processability and thermomechanical properties of stereocomplexable polylactide-based materials. ACS Appl Mater Interfaces 5:11797–11807
8. Hirota S, Sato T, Tominaga Y, Asai S, Sumita M (2006) The effect of high-pressure carbon dioxide treatment on the crystallization behavior and mechanical properties of poly(l-lactic acid)/poly(methyl methacrylate) blends. Polymer 47:3954–3960
9. Eguiburu JL, Iruin JJ, Fernandez-Berridi MJ, Roman JS (1998) Blends of amorphous and crystalline polylactides with poly(-methyl methacrylate) and poly(methyl acrylate): a miscibility study. Polymer 39:6891–6897
10. Shirahase T, Komatsu Y, Tominaga Y, Asai S, Sumita M (2006) Miscibility and hydrolytic degradation in alkaline solution of poly(l-lactide) and poly(methyl methacrylate) blends. Polymer 47:4839–4844
11. Yao B, Nawaby AV, Liao X, Burk R (2007) Physical characteristics of PLLA/PMMA blends and their CO_2 blowing foams. J Cell Plast 43:385–398
12. Li S-H, Woo EM (2008) Immiscibility–miscibility phase transitions in blends of poly(L-lactide) with poly(methyl methacrylate). Polym Int 57:1242–1251
13. Li S-H, Woo EM (2008) Effects of chain configuration on UCST behavior in blends of poly(L-lactic acid) with tactic poly(methyl methacrylate)s. J Polym Sci B 46:2355–2369
14. Canetti M, Cacciamani A, Bertini F (2014) Miscible blends of polylactide and poly(methyl methacrylate): morphology, structure, and thermal behaviour. J Polym Sci B 52:1168–1177
15. Samuel C, Raquez J-M, Dubois P (2013) PLLA/PMMA blends: a shear-induced miscibility with tunable morphologies and properties? Polymer 54:3931–3939
16. Velascoa D, Benitoa L, Fernández-Gutiérrez M, San Romána J, Elvira C (2010) Preparation in supercritical CO_2 of porous poly(methyl methacrylate)-poly(L-lactic acid) (PMMA-PLA) scaffolds incorporating ibuprofen. J Supercrit Fluids 54:335–341
17. Yoon Y, Plummer CJG, Thoemen H, Månson J-AE (2014) Liquid CO_2 processing of solid polylactide foam precursors. J Cell Plast. doi:10.1177/0021955X14537662
18. Fischer EW, Sterzel HJ, Wegner G (1973) Investigation of the structure of solution grown crystals of lactide copolymers by means of chemical reaction. Kolloid-Zu Z-Polymer 251:980–999
19. Brostow W, Chiu R, Kalogeras IM, Vassilikou-Dova A (2008) Prediction of glass transition temperatures: binary blends and copolymers. Mater Lett 62:17–18
20. Herrera D, Zamora JC, Bello A, Grimau M, Laredo E, Müller AJ, Lodge TP (2005) Miscibility and crystallization in polycarbonate/poly(epsiloncaprolactone) blends: application of the self-concentration model. Macromolecules 38:5109–5117
21. Breckner MJ, Schneider HA, Cantow H-J (1988) Approach to the composition dependence of the glass transition temperature of compatible polymer blends. Polymer 29:78–85
22. Lodge TP, McLeish TCB (2000) Self-concentrations and effective glass transition temperatures in polymer blends. Macromolecules 33:5278–5284
23. Grijpma DW, Penning JP, Pennings AJ (1994) Chain entanglement, mechanical properties and drawability of poly(lactide). Colloid Polym Sci 272:1068–1081
24. Subramanian V, Samuel Asirvatham P, Balakrishnan R, Ramasami T (2001) Molecular mechanics studies on polypropylene and polymethylmethacrylate polymers. Chem Phys Lett 342:603–609
25. Chow ST (1980) Molecular interpretation of glass transition temperature of polymer-diluent systems. Macromolecules 364:362–364
26. Plummer CJG, Yonghoon Y, Garin L, Månson J-AE (2015) Crystallization of polylactide during impregnation with liquid CO_2. Polym Bull 72:103–116
27. Krause B, Diekmann K, van der Vegt NFA, Wessling M (2002) Open nanoporous morphologies from polymeric blends by carbon dioxide foaming. Macromolecules 35:1738–1745
28. Yu F, Liu T, Zhao X, Yu X (2012) Effects of talc on the mechanical and thermal properties of polylactide. J Appl Polym Sci 125:E99–E109
29. Bhattacharya S, Gupta RK, Bhattacharya SN (2010) Role of clay in compatibilization of immiscible high melt strength polypropylene and ethylene vinyl acetate copolymer blends. Polym Eng Sci 50:1350–1357
30. Witt MRJ, Shah S (2008) Methods of manufacture of polylactic acid foams, WO 2008/093284 A1
31. Gibson LJ, Ashby MF (1999) Cellular solids: structure and properties, 2nd edn. Cambridge University Press, Cambridge